# Mesoscale Finite Element Modelling of Failure Behaviour of Steel-bar Reinforced UHPFRC Beams with Randomly Distributed Fibres

Y. Zhang[1,*], Z. Yang[1], N. Tsang[2]

[1] Centre for Built and Natural Environment, Faculty of Engineering and Computing, Coventry University, Coventry, UK.
zhang278@uni.coventry.ac.uk; ac1098@coventry.ac.uk
[2] School of Energy, Construction and Environment, Coventry University, Coventry, UK.
aa8607@coventry.ac.uk

## Abstract

This study develops a nonlinear finite element model for simulation of complicated failure behaviour of ultra high performance fibre reinforced concrete (UHPFRC) beams reinforced with steel bars and stirrups. In this model, the continuum damage plasticity model is used as the constitutive law for the UHPC matrix, and cohesive elements are used to simulate the softening bond-slip behaviour of the steel fibres/bars – UHPC matrix interfaces. Both the steel fibres and bars are modelled by elastic-plastic beam elements. As such, all the potential failure modes, including the matrix cracking and crushing, yielding and breakage of steel bars and fibres, and debonding of interfaces, can be simulated. A beam under four-point loading with various shear span versus beam depth ratios was simulated to validate the model. The results were compared well with experiments in terms of load-deflection curves and failure behaviour.

**Key words:** *Concrete; UHPFRC; Mesoscale Finite Element Model; Damage Plasticity Model; Cohesive Elements.*

## 1. Introduction

The ultra high performance fibre reinforced concrete (UHPFRC) is a relatively new cementitious composite material with much higher strength, toughness and durability than the normal-strength concrete, high-performance concrete and fibre reinforced concrete [1]. These superior properties are achieved using high strength steel fibres (>2000MPa), low water/binder ratios (<0.2), fine sands (<0.5mm), micro-silica fume and superplasticizers [2]. The use of UHPFRC allows designers to select lighter sections and longer spans for structural members [3], and makes partial or complete removal of conventional steel bars possible with improved durability and loading capacity [4].

However, the application of reinforced UHPFRC beams in engineering practice is still limited, mainly due to high materials' costs, in particular from the steel fibres. Another reason is that the structural performance is heavily affected by the distribution and orientation of fibres, which are dependent on casting procedures. This has been confirmed by limited computed tomography (CT) scanning [5] and [6]. However, such experimental investigation of the fibre distribution and orientation in large-sized structural members is difficult. Numerical modelling studies of structural behaviour of reinforced UHPFRC beams are very limited and most of them assumed homogenised macroscopic constitutive relations without explicitly modelling the fibres [7-8]. The effects of fibre distribution and orientation



This paper develops 2D mesoscale nonlinear finite element (FE) models to simulate the failure behaviour of UHPFRC beams reinforced with steel bars, with explicit simulation of random distributed fibres and the nonlinear bond-slip behaviour of steel fibres/bars – UHPC matrix interfaces. As such, the crack initiation and propagation, the softening load-displacement curves and the ultimate failure patterns can all be simulated and compared with the experimental data.

## 2. Finite element models

A reinforced UHPFRC beam consists of UHPC matrix, steel fibres, steel bars, fibre-matrix interfaces and bar-matrix interfaces. The matrix is modelled by four-noded isoparametric elements (CPS4R). The randomly distributed fibres are generated using a MATLAB code. Both the fibres and steel bars are

modelled as two-noded Timoshenko beam elements (B21) considering bending resistance. The interfaces are modelled as zero-thickness cohesive elements (COH2D4) which are inserted between the steel fibres/ bars and the matrix by a MATLAB code. The cohesive elements are inserted in a unique way that all the fibres and steel bars can deform in the plane but appear to be 'floating' on the matrix (Fig. 1). This avoids using very fine local meshes in the matrix surrounding the thin fibres and steel bars as well as embedding the fibres/bars in the matrix, a simplified but unrealistic assumption used in most existing mesoscale studies [9].

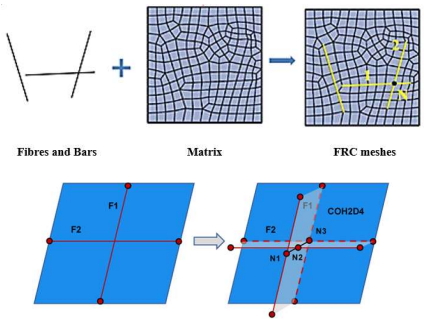


Fig. 1 The FE model: mesh generation (top) and cohesive elements (bottom)

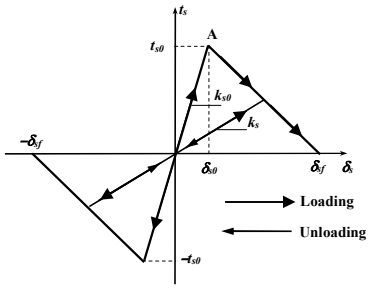


Fig. 2 Softening behaviour of cohesive elements for interfacial bond-slip

The elastoplastic constitutive laws are used to model steel fibres and bars with yielding, strain hardening and rupture. The concrete damage plasticity (CDP) model in ABAQUS is used for the UHPC matrix. The pre-peak behaviour is assumed as linear elastic for both compression and tension. The post-peak softening compressive behaviour is described by the compressive stress ($\sigma_c$) - strain ($\varepsilon_c$) curve suggested by Guo [10]. The UHPC's tensile behaviour is described by a traction ($\sigma_t$) - crack opening displacement (w) curve to minimize the mesh dependence of results [11].The linear shear traction ($t_s$) - slip ($\delta_s$) curve shown in Fig. 2 is used as the constitutive law of cohesive elements to simulate the softening bond-slip behaviour of the interfaces. The normal traction $t_n$ is assumed as ten times of the shear traction $t_s$, to model the tight surrounding mechanism of fibres by the matrix and to prevent penetration.

The four-point loaded UHPFRC beams in Fig. 3 were tested by Bahij et al. [12] with a few shear span ($a$) to depth ($d$) ratios. Beams with $a/d$=1.8 and 2.6 were modelled.

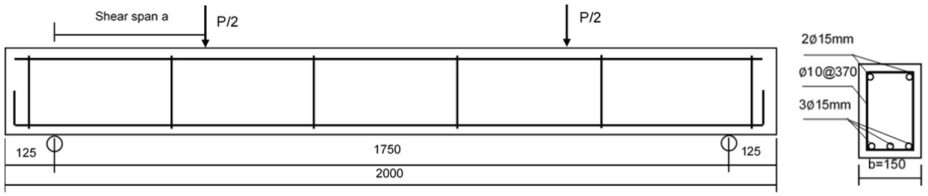


Fig. 3 Details of the reinforced UHPFRC beam [12].

2D FEM models of 1mm thickness were built. Only half the beam was modelled due to symmetry. Based on the 1% volume fraction, 0.22mm diameter and 13mm length of fibres, 3471 fibres were randomly generated and distributed in the model, as seen in Fig. 4. There are 101,869 elements for the UHPC matrix (element size 2mm, too small to be distinguishable), 14,327 cohesive elements on the interfaces, 14,327 beam elements for the fibres and steel bars, and 86,034 nodes in total. The load was applied as a vertical displacement at the two loading points. The ABAQUS/Explicit solver was used with a total time of 1s, which was found long enough to ensure the quasi-static loading condition.

The UHPC matrix has a compressive strength of 130MPa and a tensile strength of 5MPa. All the other material properties are summarised in Table 1.

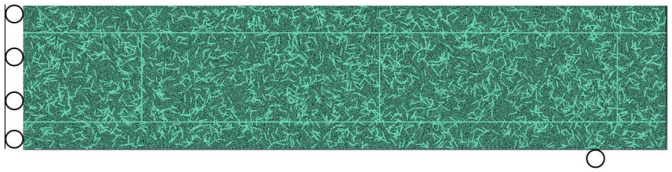

Fig. 4 The meso-scale FE model

Table 1. Material parameters

| Property | Steel fibres | Main steel bars | Stirrups | UHPC matrix | Steel fibre-matrix interfaces | Steel bar-matrix interfaces |
|---|---|---|---|---|---|---|
| **Young's modulus $E$ (GPa)** | 200 | 200 | 200 | 37 | 10 | 20 |
| **Poisson ratio $\nu$** | 0.3 | 0.3 | 0.3 | 0.19 | 0.3 | 0.3 |
| **Density $\rho$ (kg/m$^3$)** | 7850 | 7850 | 7850 | 2100 | 2100 | 2100 |
| **Yielding strength $f_y$ (MPa)** | 2500 | 1320 | 430 | - | - | - |
| **Rupture strength $f_b$ (MPa)** | 2800 | | | | | |
| **Rupture strain $\varepsilon_b$** | 0.1 | | | | | |
| **Diameter $D_f$ (mm)** | 0.22 | 15 | 10 | - | - | - |
| **Shear traction $t_s$ (MPa)** | - | - | - | - | 5 | 10 |

## 3. Numerical simulation results

### 3.1 Load-deflection responses

The load-deflection curves from the simulations are compared with the experimental results in Figs. 5 and 6. There is a good agreement overall, especially the peak loads (max 1% difference), although the numerical results are slightly stiffer at the elastic stage.

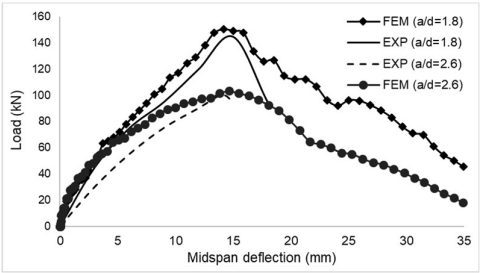


Fig. 5 Shear force-midspan deflection curves

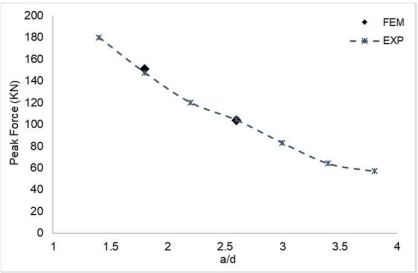


Fig. 6 Curves of peak loads verse *a/d* ratios

### 3.2 Failure behaviour

Fig. 7 and Fig. 8 shows the contours of scalar stiffness damage degradation (SDEG) in the matrix at ultimate failure, for *a*/*d*=1.8 and 2.6, respectively, compared with the experimental failure pattern. An overall good agreement can be seen for both beams, particularly for *a*/*d*=1.8, including the diagonal crack propagation in the shear span, the flexural crack propagation in the bending span, the horizontal crack propagation along the main bars etc.

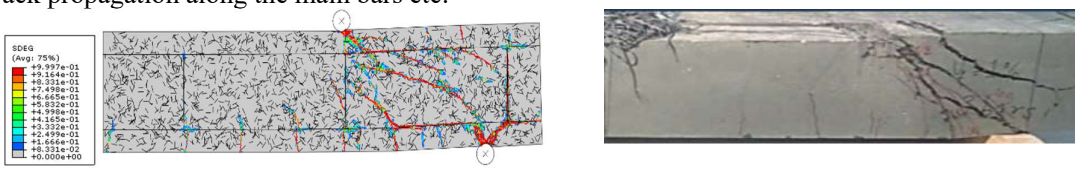

Fig. 7 Failure patterns of reinforced UHPFRC beams with *a*/*d*=1.8: simulated (left) and tested (right)

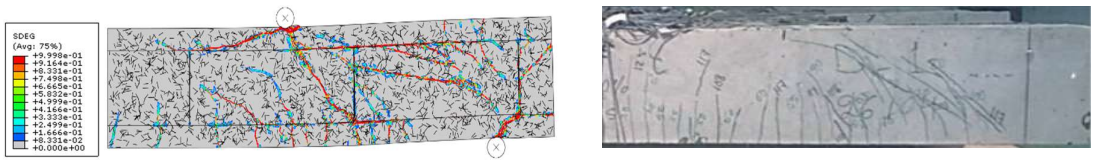

Fig. 8 Failure patterns of reinforced UHPFRC beams with *a*/*d*=2.6: simulated (left) and tested (right)

## 4. Conclusions

2D nonlinear mesoscale FE models have been developed to simulate the complete failure process of reinforced UHPFRC beams. Combing the continuum CDP model for the UHPC matrix, the discrete cohesive elements for the fibres/bars-matrix interfaces and the elastoplastic models for fibres and bars, all the failure modes such as the matrix fracture and spalling, interfacial bond-slip, fibre yielding and rupture are modelled. Reinforced UHPFRC beams with different shear span-depth ratios were simulated and the results are in good agreement with experimental data. The mesoscale models allow for further parametric studies of key material and structural factors, such as the volume fraction, distribution and orientation of fibres, the reinforcement arrangement and ratio, the shear span ratio etc, so as to optimise these factors for desired mechanical properties with minimum material cost.

## Acknowledgements

The first author would like to thank the financial support of a full PhD studentship from Coventry University.

## References

[1] Richard P., & Cheyrezy M., Composition of reactive powder concretes. Cem. Concr. Res., 25(7) (1995) 1501-1511.
[2] Wille K., Naaman A.E., El-Tawil S., & Parra-Montesinos G.J., Ultra-high performance concrete and fibre reinforced concrete: achieving strength and ductility without heat curing. Mater. Struct., 45(3) (2012) 309-324.
[3] Shah A.A., & Ribakov Y., Recent trends in steel fibred high-strength concrete. Mater. Des., 32(8) (2011) 4122-4151.
[4] Li V.C., Ward R. & Hamza A.M., Steel and synthetic fibres as shear reinforcement. ACI Mater. J., 89 (5) (1992) 499-508.
[5] Barnett S.J., Lataste J.F., Parry T., Millard S.G., Soutsos M.N., Assessment of fibre orientation in ultra high performance fibre reinforced concrete and its effect on flexural strength, Mater. Struct. 43 (7) (2010) 1009-1023.
[6] Qsymah A., Sharma R., Yang Z., Margetts L., Mummery P., Micro X-ray computed tomography image-based two-scale homogenisation of ultra high performance fibre reinforced concrete, Constr. Build. Mater. 130 (2016) 230-240.
[7] Schramm N., Fischer O., Investigations on the shear behaviour of bridge girders made of normal and ultra-high performance fiber-reinforced concrete. Proc. Eng., 156 (2016) 411-418.
[8] Yoo D.Y. and Yoon Y.S., Structural performance of ultra-high performance concrete beams with different steel fibers. Eng. Struct., 102 (2015) 409-423.
[9] Zhang H., Huang Y.J., Yang Z.J., Xu S.L., Chen X.W., A discrete-continuum coupled finite element modelling approach for fiber reinforced concrete, Cem. Concr. Res., 106 (2018) 130-143.
[10] Guo Z.H., Concrete strength and constitutive relation: Principle and Application, China Architecture and Building Press, Beijing, 2004.
[11] Hordijk D.A., Tensile and tensile fatigue behaviour of concrete; experiments, modelling and analyses, Heron, 37 (1992) 1-79.
[12] Bahij S., Adekunle SK., Al-Osta M., Ahmad S., Al-Dulaijan SU., Rahman M., Numerical investigation of the shear behaviour of reinforced ultra-high-performance concrete beams. Struct. Concr., 19 (2018) 305-317